



Thermo-mechanical and optical properties of calcium aluminosilicate glasses doped with Er^{3+} and Yb^{3+}

J.A. Sampaio ^a, T. Catunda ^a, A.A. Coelho ^b, S. Gama ^b, A.C. Bento ^c,
L.C.M. Miranda ^c, M.L. Baesso ^{c,*}

^a Instituto de Física de São Carlos, Universidade de São Paulo, 13560-250 São Carlos, SP, Brazil

^b Instituto de Física Gleb Wataghin, Universidade Estadual de Campinas, 13083-970 Campinas, SP, Brazil

^c Departamento de Física, Universidade Estadual de Maringá, Av. Colombo 5790, 87020-900 Maringá, PR, Brazil

Abstract

In this work a series of Er_2O_3 and Yb_2O_3 doped and Er_2O_3 – Yb_2O_3 co-doped low silica calcium aluminosilicate glasses have been melted at 1470°C under vacuum conditions. Measurements of optical absorption coefficient, mass density, refractive index, Vickers micro-hardness, glass transformation temperature (T_g) and crystallization temperature (T_x) have been carried out. The results showed that these glasses dissolved ~ 1.5 mol% Er_2O_3 and ~ 1.1 mol% Yb_2O_3 in their structure without devitrification and also that only small changes ($\sim 10\%$) have been measured in their thermal, mechanical and optical properties. © 2000 Elsevier Science B.V. All rights reserved.

1. Introduction

Recently, the emission of light at 2.8 μm from an oxide glass has been successfully observed [1]. The glass was low silica content calcium aluminosilicate glasses doped with erbium and ytterbium. The idea behind the use of rare earth (RE) co-doping is to take advantage of the fact that Yb^{3+} acts as sensitizer for Er^{3+} , a mechanism which has been known for a long time [2]. Light sources in the 2.8 μm region are of particular interest for medical applications due to the water absorption in this spectral region [3], as well as for communications and chemical sensor device [4]. In the case of high power laser applications in hostile

environments, restricting limitations are usually imposed on the glass host material to be used [5,6]. The hosts should have high thermal conductivity, high glass transformation temperatures (T_g), good thermal shock resistance, good chemical durability, high fluorescence quantum efficiency and low phonon energies. Amongst the several glass systems, low silica content calcium aluminosilicate glasses have been shown to fulfill most of these restricting requirements [7–11], besides being non-toxic that is important for surgical laser applications [12].

Despite such properties, only recently to our knowledge, RE doped low silica calcium aluminosilicate glasses attracted the attention of several investigators [1,10,13–20], probably due to the tendency of these glasses towards devitrification, since they are formed with non-network formers CaO and Al_2O_3 [9]. The addition of small amounts of alkali and alkaline earth elements enlarges the

* Corresponding author. Tel.: +55-44 261 4330; fax: +55-44 263 4242.

E-mail address: mlbaesso@dfi.uem.br (M.L. Baesso).

glass forming region, and samples of about 5.5 kg can be produced [21]. Several calcium aluminate glasses compositions containing silica, magnesium and barium oxide have been investigated by Davy [7] and optimized glass compositions are now reported in the literature [22–27]. Nevertheless, few papers to our knowledge have been devoted to the investigation of low silica calcium aluminosilicate glasses doped with RE ions. And even so most of them were concerned with the investigation of spectroscopic properties such as quantum efficiency, energy transfer process, mechanism of up-conversion [1,10,11,13–18,20]. So, little information is available about the affect of RE doping on their optical, thermal and mechanical properties.

In this work we investigate the affect of RE doping of low silica content calcium aluminosilicate glasses on their mass density (ρ), Vickers micro-hardness (H_v), optical absorption coefficient (α), refractive index, glass transition temperature (T_g) and glass crystallization onset temperature (T_x).

2. Experimental

The low silica calcium aluminosilicate glass samples were prepared from reagent grade powder CaCO_3 (99%), Al_2O_3 (99.1%), SiO_2 (99%), MgO (97%), Er_2O_3 (99.99%) and Yb_2O_3 (99.99%). The sample compositions are listed in Table 1. A batch was melted at 1470°C in 30 g quantities under vacuum conditions (10^{-3} bar) in a graphite crucible for 2 h for fining. The liquid was cooled by switching off the heater and then moving the crucible upward in the vacuum chamber to a region at room temperature. The sample annealing was carried out at a heating rate of 10°C/min to a few degrees $<T_g$, the glass transition temperature, and remained at this temperature for 12 h, before cooling to room temperature. All glasses were examined for crystallinity with optical microscopy and X-ray diffraction. The samples were cut with a slow speed saw in two different shapes. 3 mm \times 3 mm \times 10 mm for optical and mechanical measurements and samples approximately 150 mg for differential thermal analyses (DTA).

The refractive index measurements were performed using a Pulfrich refractometer (JENA DDR) at six different wavelengths: mercury *H* band (404.7 nm), mercury *g* band (435.8 nm), hydrogen *F* band (486.1 nm), mercury *e* band (546.7 nm), helium *d* band (587.6 nm) and hydrogen *C* band (656.3 nm). The density measurements were carried out using the Archimedes buoyancy method with CCl_4 (density 1.594 g/cm³ at 20°C) as the immersion liquid. Vickers micro-hardness were performed using a micro-hardness tester (Leitz Wetzlar) with 200 g load during 15 s. To minimize experimental errors, at least 15 indentations were recorded. DTA analysis was performed using an equipment (Netzsch, STA 409 – EP), at a heating rate of 10°C/min until 1400°C, in an alumina crucible. Optical absorption spectra were recorded on a spectrophotometer (Perkin–Elmer Lambda 9) at room temperature.

3. Results

For the doped glasses the limit of vitrification was found at a maximum of ~ 1.5 mol% of RE oxide. In the samples so obtained, observed by optical microscopy, we detected no bubbles striae, as well as no evidence of crystallization in the X-ray diffractograms. The optical absorption spectra of a Yb^{3+} and Er^{3+} doped sample are shown in Figs. 1(A)–(C), in which the assignment of the typical Er^{3+} and Yb^{3+} transition [28] are indicated. Density (ρ), Vickers micro-hardness (H_v), glass transition temperature (T_g), glass crystallization onset temperature (T_x), mean molecular mass \bar{M} calculated from the relation $\bar{M} = \sum_i x_i M_i$, where x_i is the mole fraction of the glass constituents and M_i is the molecular mass of the glass constituents and the molar volume, $\bar{V} = \bar{M}/\rho$, are summarized in Table 1. The affect of composition on the density is shown in Fig. 2. The density increased linearly as the RE oxide replaced alumina, from 2.928 ± 0.005 g/cm³ for undoped sample to 3.123 ± 0.005 for the 1.48 ± 0.05 mol% Er_2O_3 doped one. The refractive index ($\pm 2 \times 10^{-5}$) as function of RE oxide concentration and wavelength are shown in Figs. 3(A) and (B), respectively. The refractive index increased linearly as

Table 1
Composition and properties of low silica content calcium aluminosilicate glasses

Sample	Composition (mol%)						ρ (g/cm ³) ±0.002	\bar{M} (g/mol) ±0.05	\bar{V} (mol/cm) ±0.05	H_v (kg/mm ²)	T_g (°C) ±3	T_x (°C) ±3
	CaO	Al ₂ O ₃	MgO	SiO ₂	Er ₂ O ₃	Yb ₂ O ₃						
CASM	58.11	27.11	6.89	7.89	–	–	2.928	67.75	23.14	865 ± 25	841	1058
CAYB1	57.77	27.15	6.95	7.96	–	0.17	2.960	68.33	23.08	837 ± 18	813	1029
CAYB3	58.35	26.06	7.02	8.04	–	0.53	3.007	69.04	22.96	814 ± 29	803	993
CAYB5	58.94	24.97	7.09	8.12	–	0.88	3.057	69.63	22.78	807 ± 24	788	982
CAER05	59.33	27.72	4.75	8.25	0.09	–	2.946	68.75	23.34	852 ± 21	821	1038
CAER1	57.94	26.99	6.94	7.95	0.18	–	2.957	68.27	23.09	831 ± 23	817	1035
CAER2	57.83	26.94	6.83	8.03	0.37	–	2.973	69.93	23.52	824 ± 19	822	1018
CAER4	58.69	25.54	6.94	8.10	0.73	–	3.027	69.50	22.96	815 ± 15	798	1000
CAER6	59.30	24.42	7.01	8.18	1.00	–	3.076	70.02	22.76	800 ± 20	791	979
CAER7	59.54	23.84	7.16	8.21	1.25	–	3.099	70.30	22.68	793 ± 19	787	958
CAER8	59.83	23.26	7.20	8.24	1.48	–	3.123	70.95	22.72	781 ± 23	782	955
CAER2YB3	58.93	24.96	7.09	8.12	0.37	0.53	3.053	69.74	22.94	785 ± 10	794	979
CAER2YB4	59.23	24.40	7.13	8.16	0.37	0.71	3.075	70.08	22.79	776 ± 22	790	976
CAYB2ER05	58.20	26.34	7.00	8.02	0.09	0.35	2.992	68.86	23.01	815 ± 14	807	1006
CAYB2ER1	58.34	26.06	7.03	8.04	0.18	0.35	3.002	69.02	22.99	811 ± 14	798	1006
CAYB2ER2	58.63	25.52	8.08	7.06	0.36	0.35	3.027	69.15	22.84	808 ± 11	792	983
CAYB2ER3	58.92	24.96	7.09	8.12	0.55	0.35	3.036	69.72	22.96	804 ± 17	798	969
CAYB2ER4	59.23	24.39	7.13	8.16	0.74	0.35	3.074	70.08	22.80	798 ± 10	791	972
CAYB2ER5	59.53	23.81	7.17	8.21	0.93	0.35	3.099	70.42	22.72	795 ± 13	785	969

RE oxide replaced alumina. The refractive index decreased with increasing wavelength. In Table 2, the refractive index as function of wavelength, average dispersion, $n_F - n_C$, Abbe number, $v_d = (n_d - 1)/(n_F - n_C)$, and molar refraction are summarized for the samples.

The molar refraction was calculated using Lorentz–Lorenz equation [29]

$$MR_g = \frac{n^2 - 1}{n^2 + 2} \frac{\bar{M}}{\rho},$$

where $n = n_d$ is the refractive index. It follows from Table 2 that MR_g remained approximately constant at 8.6. The dependence H_v on the RE oxide doping was such that H_v decreased as Al₂O₃ was replaced by the RE oxide, as shown in Fig. 4. Furthermore, this change in H_v is independent of the RE doping, which we suggest is due to the alumina which we assume has the largest affect on H_v . Fig. 5 shows the DTA curves for four samples, namely, undoped, 0.09 mol%, 0.73 mol%, 1.48 mol% Er₂O₃ doped samples. Increasing the RE oxide doping shifts the exothermal peaks and T_g

towards smaller temperatures. This shift was observed for all samples. The dependence of T_g and T_x on the RE oxide doping concentration are shown in Fig. 6, which shows that both T_g and T_x decrease as the RE oxide doping concentration increases. Finally, Figs. 7(A) and (B) show the dependence of T_g as function of specific volume and of H_v as function of density, respectively. Data for $T_g(1/\rho)$ and $H_v(\rho)$ can be fit by linear functions with correlation coefficients, $RT_g = 0.95$ and $RH_v = 0.87$.

4. Discussion

It is well-known that RE ions can act either as a network former (as in the case of fluorozirconate glasses) [30] or as a modifier (as in the case of fluoride glasses) [31,32].

The above results indicate that the addition of Er, Yb and Er–Yb ions in amounts <1.48 mol% to low silica calcium aluminosilicate glasses changes by <10% the glass properties. The density increase

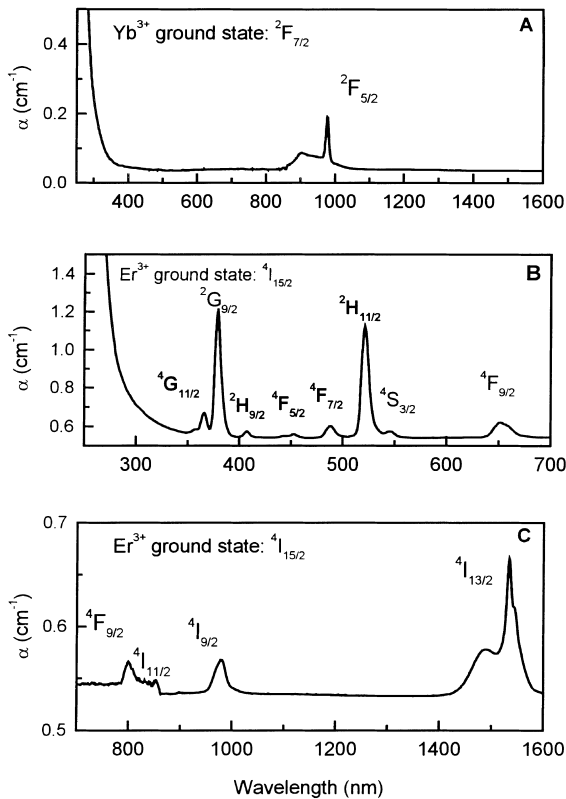


Fig. 1. Visible and IR optical absorption spectra: (A) 0.53 mol% Yb_2O_3 doped sample (2.6 mm); (B) 0.73 mol% Er_2O_3 doped sample (3.0 mm); (C) 0.73 mol% Er_2O_3 doped sample near infrared.

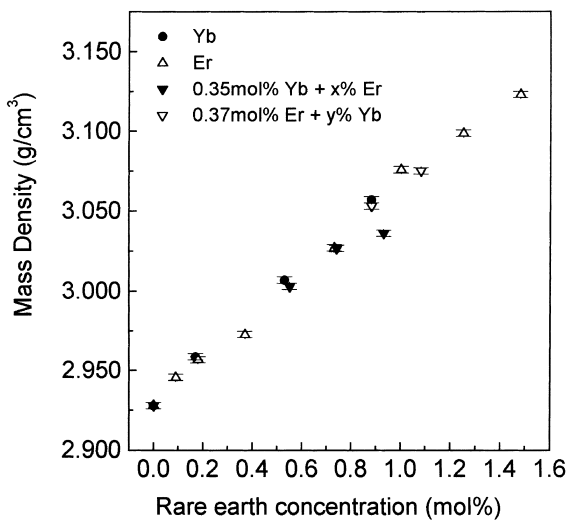


Fig. 2. Mass density as a function of RE oxide concentration.

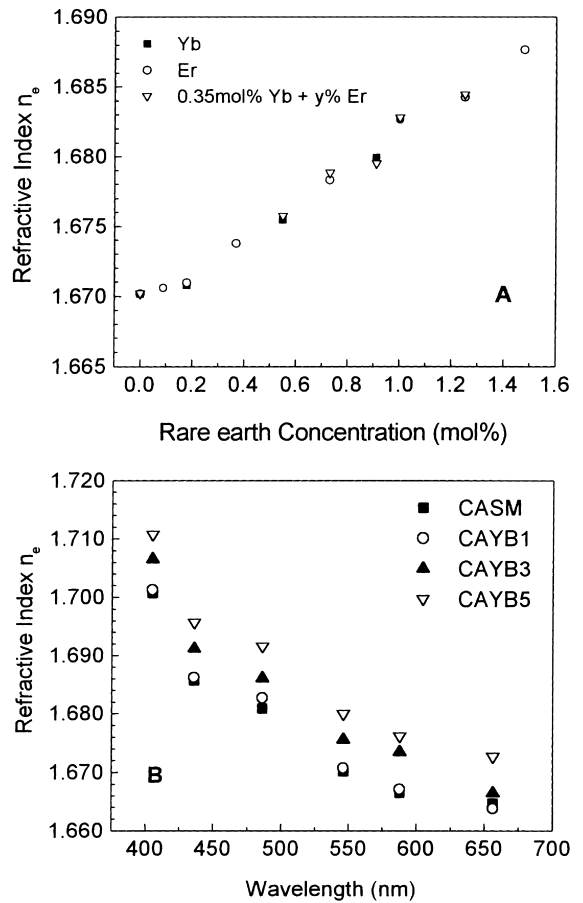


Fig. 3. (A) Refractive index at 546.07 nm as a function of RE oxide concentration; (B) refractive index as a function of wavelength for Yb_2O_3 doped samples.

as a function of RE oxide concentration is explained by the relative masses of RE ions in comparison with Al, which it replaces. The increase of the refractive index, between the un-doped sample and the 1.48 mol% Er_2O_3 doped sample was of the order of 1%, in accordance with previously reported results [25,26]. As discussed in previous works [25,32] the ratio $\text{Al}_2\text{O}_3/\text{CaO}$ affects the structural properties of these glasses. According to this structural model [25,32] non-bridging oxygen (NBO) occurs when the $\text{Al}_2\text{O}_3/\text{CaO}$ ratio is less than 1. In the case of the sample undoped this ratio is 0.466 and 0.388 for 1.48 mol% Er_2O_3 doped one, i.e., as alumina is replaced by the RE oxide there is a decrease of about 20% in the

Table 2
Refractive index dependence of RE doping in low silica calcium aluminosilicate glasses

Sample	<i>H</i> 404.7 nm	<i>g</i> 435.8 nm	<i>F</i> 486.1 nm	<i>e</i> 546.07 nm	<i>d</i> 587.6 nm	<i>C</i> 656.3 nm	$n_F - n_C$ ($\times 10^{-3}$) ± 0.02	v_d ± 0.03	MR_g (cm^3) ± 0.06
CASM	1.70073	1.68562	1.68088	1.67015	1.66647	1.66100	19.87	33.53	8.61
CAYB1	1.70121	1.68620	1.68266	1.67075	1.66708	1.66381	18.85	35.39	8.59
CAYB3	1.70647	1.69113	1.68605	1.67545	1.67342	1.66644	19.61	34.35	8.61
CAYB5	1.71071	1.69568	1.69158	1.67992	1.67609	1.67264	18.94	35.70	8.57
CAER05	1.70121	1.68586	1.68239	1.67056	1.66673	1.66337	19.03	35.04	8.68
CAER1	1.70159	1.68639	1.68257	1.67093	1.66732	1.66399	18.58	35.92	8.60
CAER2	1.70258	1.68739	1.68302	1.67375	1.66838	1.66455	18.46	36.20	8.77
CAER4	1.70763	1.69248	1.68797	1.67829	1.67458	1.66761	20.36	33.14	8.62
CAER6	1.71203	1.69679	1.69292	1.68264	1.67669	1.67327	19.65	34.43	8.57
CAER7	1.71573	1.70047	1.69506	1.68422	1.68225	1.67518	19.88	34.33	8.59
CAER8	1.71900	1.70396	1.69720	1.68763	1.68398	1.67689	20.30	33.69	8.62
CAER2YB3	1.71090	1.69582	1.69167	1.67996	1.67587	1.67242	19.25	35.11	8.59
CAER2YB4	1.71099	1.69564	1.69274	1.68018	1.67676	1.67322	19.52	34.67	8.58
CAYB2ER05	1.70601	1.69094	1.68471	1.67523	1.67293	1.66589	18.82	35.75	8.63
CAYB2ER1	1.70647	1.69136	1.68578	1.67572	1.67422	1.66716	18.62	36.20	8.63
CAYB2ER2	1.71003	1.69472	1.68708	1.67882	1.67467	1.66769	19.38	34.81	8.58
CAYB2ER3	1.71026	1.69522	1.69194	1.67948	1.67604	1.67255	19.38	34.88	8.64
CAYB2ER4	1.71231	1.69702	1.69292	1.68277	1.67732	1.67377	19.14	35.38	8.59
CAYB2ER5	1.71591	1.70070	1.69515	1.68444	1.68222	1.67518	19.96	34.17	8.61

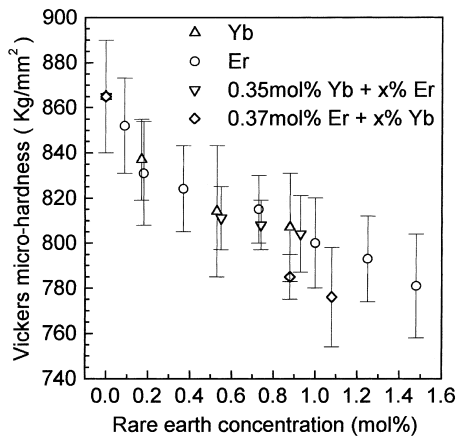


Fig. 4. Vickers micro-hardness for different RE oxide concentration.

$\text{Al}_2\text{O}_3/\text{CaO}$ ratio. As a consequence there is an increase of the NBO in the samples, which, in turn, entails an increase of their polarizability. As a result of this increase in polarizability the refractive index should also increase [33].

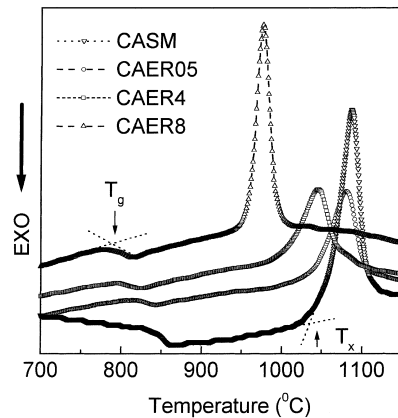


Fig. 5. DTA curves showing the shift of thermal events (T_g and T_x) towards smaller temperatures.

The decrease of H_v was of the order of 10%. This decrease is explained assuming that the RE ions disrupt the tetrahedral network, thereby decreasing the network connectivity. We explain the decrease of T_g by about 59°C in the 1.48 mol% Er_2O_3 doped one by assuming that the RE–O

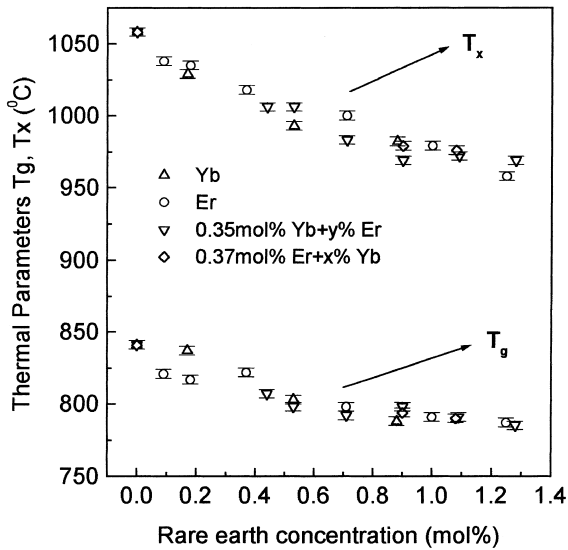


Fig. 6. Thermal parameters T_x and T_g as Al_2O_3 is replaced by RE oxide.

bonds are weaker than aluminum–oxygen bonds. As discussed by Shelby and Siliaty [25] the replacement of Al_2O_3 by Ga_2O_3 causes a decrease of T_g based on smaller strength of Ga_2O_3 bonding compared to Al_2O_3 . As RE cations have smaller field strength as compared to Al, we assume that the connectivity of the glass structure decreases, requiring less thermal energy for the movement of the less connected structural units and decreasing viscosity. Although the temperature range, between T_x and T_g (in which the case of our samples is around 190°C), as discussed in previous works [27,32], this parameter is not entirely reliable for predicting glass stability, since the sample compositions investigated are in the range close to a phase diagram limit. Finally, from linear fitting $T_g(1/\rho)$ and $H_v(\rho)$ we conclude that the changes in the glass network induced by RE doping affects H_v and T_g in a similar manner.

5. Conclusion

The results showed that these glasses allowed the inclusion of a considerable amount of RE oxide (<2.0 mol%) without devitrification and had only small changes in properties such as mass

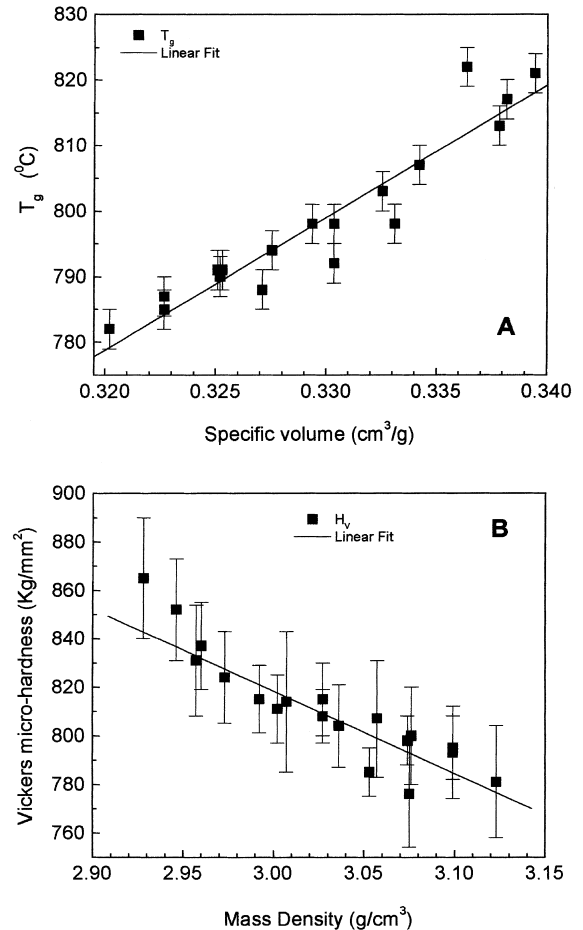


Fig. 7. (A) T_g as a function of specific volume; (B) Vickers micro-hardness as a function of mass density. Solid curve represents linear regression.

density, refractive index, micro-hardness and T_g . There was an increase of density by approximately 7%, and refractive index of the order of 1%. In contrast, the Vickers micro-hardness and T_g decreased approximately 9% and 7%, respectively, from undoped to the 1.48 mol% Er_2O_3 doped sample. Based on our results we suggest that RE^{3+} ion act as modifiers in the structure of the low silica calcium aluminosilicate glasses investigated in this work. Since the changes in the main physical properties of these glasses was $<10\%$, we suggest they should be considered as candidates for active media in the development of glass lasers.

Acknowledgements

We are thankful to Brazilian Agencies: Capes, CNPq and FAPESP for the financial support of this work.

References

- [1] D.F. de Souza, L.F.C. Zonetti, M.J.V. Bell, J.A. Sampaio, L.A.O. Nunes, M.L. Baesso, A.C. Bento, L.C.M. Miranda, *Appl. Phys. Lett.* 74 (1999) 908.
- [2] F.E. Auzel, *Proc. IEEE* 61 (1973) 758.
- [3] R.M. Dwyer, M. Bass, in: M. Ross (Ed.), *Lasers in Medicine*, vol. 3, Academic Press, New York, 1977, p. 107.
- [4] K. Kincade, *Laser Focus World* (1996) 73.
- [5] N. Neuroth, *Opt. Eng.* 26 (1987) 96.
- [6] M.J. Weber, *J. Non-Cryst. Solids* 123 (1990) 208.
- [7] J.R. Davy, *Glass Technol.* 19 (1978) 32.
- [8] G.Y. Onoda Jr., S.D. Brown, *J. Am. Ceram. Soc.* 53 (1970) 311.
- [9] J.E. Shelby, *J. Am. Ceram. Soc.* 68 (1985) 155.
- [10] M.L. Baesso, A.C. Bento, A.R. Duarte, A.M. Neto, L.C.M. Miranda, J.A. Sampaio, T. Catunda, S. Gama, F.C.G. Gandra, *J. Appl. Phys.* 85 (1999) 8112.
- [11] S. Tanabe, T. Ohyagi, T. Hanada, N. Soga, *J. Ceram. Soc. Jpn.* 101 (1993) 74.
- [12] T. Abel, J.A. Harrington, P.R. Foy, *Appl. Opt.* 33 (1994) 3919.
- [13] X. Zou, T. Izumitani, *J. Non-Cryst. Solids* 162 (1993) 68.
- [14] X. Zou, T. Izumitani, *J. Ceram. Soc. Jpn.* 101 (1993) 80.
- [15] X. Zou, T. Izumitani, *J. Ceram. Soc. Jpn.* 101 (1993) 85.
- [16] M.L. Baesso, A.C. Bento, A.A. Andrade, T. Catunda, J.A. Sampaio, S. Gama, *J. Non-Cryst. Solids* 219 (1997) 165.
- [17] M.L. Baesso, A.C. Bento, A.A. Andrade, J.A. Sampaio, E. Pecoraro, L.A.O. Nunes, T. Catunda, S. Gama, *Phys. Rev. B* 57 (1998) 10545.
- [18] E.V. Uhlmann, M.C. Weinberg, N.J. Kreidl, L.L. Burgner, R. Zaroni, K.H. Church, *J. Non-Cryst. Solids* 178 (1994) 15.
- [19] J.A. Sampaio, T. Catunda, F.C.G. Gandra, S. Gama, A.C. Bento, L.C.M. Miranda, M.L. Baesso, *J. Non-Cryst. Solids* 247 (1999) 196.
- [20] W.J. Chung, J.R. Yoo, Y.S. Kim, J. Heo, *J. Am. Ceram. Soc.* 80 (1997) 1485.
- [21] H.C. Hafner, N.J. Kreidl, R.A. Weidel, *J. Am. Ceram. Soc.* 41 (1958) 315.
- [22] C. Huang, E.C. Behrman, *J. Non-Cryst. Solids* 128 (1991) 310.
- [23] C. Oprea, D. Togan, C. Popescu, *Thermochim. Acta* 194 (1992) 165.
- [24] E.V. Uhlmann, M.C. Weinberg, N.J. Kreidl, A.A. Goktas, *J. Am. Ceram. Soc.* 76 (1993) 499.
- [25] J.E. Shelby, R.M. Slilaty, *J. Appl. Phys.* 68 (1990) 3207.
- [26] J.E. Shelby, M.M. Wierzbicki, *Phys. Chem. Glasses* 36 (1995) 17.
- [27] P.L. Higby, R.J. Ginther, I.D. Aggarwal, E.J. Friebele, *J. Non-Cryst. Solids* 126 (1990) 209.
- [28] W.T. Carnall, P.R. Fields, K. Rajnak, *J. Chem. Phys.* 49 (1968) 2212.
- [29] W. Vogel, *Glass Chemistry*, 2nd Ed., Springer, Berlin, 1994, p. 411.
- [30] L. Lucas, M. Chasnthanasinh, M. Poulain, P. Brun, M.J. Weber, *J. Non-Cryst. Solids* 27 (1978) 273.
- [31] J.E. Shelby, J.T. Kohli, *J. Am. Ceram. Soc.* 73 (1990) 39.
- [32] J.T. Kohli, J.E. Shelby, *Phys. Chem. Glasses* 32 (1991) 67.
- [33] J.E. Shelby, C.M. Shaw, M.S. Spess, *J. Appl. Phys.* 66 (1989) 1149.